

Article

Photocatalytic Degradation of Organic Dyes from Clinical Laboratory Wastewater

J. H. Ramírez Franco ^{1,*}, S. D. Castañeda Cárdenas ² and H. R. Zea Ramírez ²

¹ Departamento de Ingeniería Química, Universidad Nacional de Colombia, Campus la Nubia, Manizales 11121, Colombia

² Departamento de Ingeniería Química y Ambiental, Universidad Nacional de Colombia, Ciudad Universitaria, Bogotá 111321, Colombia

* Correspondence: jhramirezfra@unal.edu.co

Abstract: Clinical laboratory wastewaters are of important environmental concern due to the highly complex chemical reagents and dyes used to identify various pathologies, which are difficult to degrade by conventional treatment methods. The present research aimed to assess the effects of ilmenite use in the discoloration process of clinical laboratory wastewater. The wastewater originates from a Gram staining process used to identify pathogenic microorganisms present in biological samples. The active ingredient is crystal violet, a triphenylmethane dye derivative, highly toxic and non-biodegradable that causes a shiny purple color in the wastewater. The ilmenite was characterized by X-ray Fluorescence, X-ray Diffraction, Scanning Electron Microscopy, energy-dispersive spectroscopy and Nitrogen adsorption isotherm, while the discoloration process of the wastewater was measured by UV–Vis spectrophotometry and pH change through the reaction time, evaluating different ilmenite loads, particle size and stability under light sources with different energies. Chemical oxygen demand analysis confirmed that acid formation and discoloration were associated with organic substance mineralization. Type C ultraviolet light and 0.7 g/L load were identified as the best operating conditions for the discoloration process. It was possible to establish that ilmenite is stable after four uses in the discoloration process, obtaining, in all cases, discoloration percentages higher than 90% after 3 h of irradiation.

Keywords: ilmenite; photocatalysis; oxidation; dyes; triphenylmethane



Citation: Ramírez Franco, J.H.; Castañeda Cárdenas, S.D.; Zea Ramírez, H.R. Photocatalytic Degradation of Organic Dyes from Clinical Laboratory Wastewater. *Water* **2023**, *15*, 1238. <https://doi.org/10.3390/w15061238>

Academic Editors: Christos S. Akrotas and Chengyun Zhou

Received: 19 January 2023
Revised: 3 March 2023
Accepted: 17 March 2023
Published: 22 March 2023



Copyright: © 2023 by the authors. Licensee MDPI, Basel, Switzerland. This article is an open access article distributed under the terms and conditions of the Creative Commons Attribution (CC BY) license (<https://creativecommons.org/licenses/by/4.0/>).

1. Introduction

Health sector comprises one of the main hazardous waste-generating activities in Colombia: in 2017 alone, 46,000 tons of hospital waste were generated [1]. Activities such as emergency care, surgery procedures, and clinical laboratory utilization, among others, produce waste that requires to be properly treated and disposed of to minimize the generation of negative environmental impacts. Waste such as medicines, dyes, and substances with high organic content are of environmental importance because they are highly polluting and difficult to degrade by conventional treatment methods.

Clinical laboratory utilization is a relevant specialty in terms of hazardous waste generation, where highly complex chemical reagents and dyes are used to identify various pathologies. One of the most commonly used techniques is the Gram stain, which uses crystal violet dye, basic fuchsin, solvents (alcohol-acetone), and lugol to identify Gram-negative bacteria in body samples. Likewise, the Ziehl–Neelsen stain uses the acid fuchsin dye, methylene blue and the same solvent for the identification of the bacteria that produce tuberculosis, and the Wright stain uses the basic methylene blue dye and the acid dye Eosin Y for the differentiation of blood cell types.

These dyes are derived from triphenylmethane, an aromatic molecule in which nitrogen is found as a radical coupled to the aromatic amines of each of the compounds,

except for eosin Y. Triphenylmethane-derived dyes are monomethine-type dyes with three aryl-type terminal systems, of which one or more are substituted with primary, secondary, or tertiary amino groups or by hydroxyl groups in the para-position relative to the methyl carbon atom. Substituents of carboxyl, sulfonic acid, halogen, alkyl, and alkoxy groups can also be found on the aromatic rings; the number, nature, and position of these substituents determine both the hue and color of the dye and the class of application to which it belongs.

Because of the complexity and toxicity related to these dyes, the main technology for their treatment involves controlled incineration, which leaves residue ashes and the emission of polluting gases. To minimize the possible environmental impacts derived from the incineration process of dye wastes, it is necessary to evaluate less impacting treatment methodologies.

In recent years, advanced oxidation processes (AOPs) have emerged as effective alternatives to treat hazardous wastes with the presence of highly polluting substances that are not very susceptible to biodegradation. These processes use oxidizing substances such as ozone and hydrogen peroxide, as well as catalysts and ultraviolet light to generate hydroxyl radicals OH^\bullet [2], super hydroxyl radicals, and other reactive oxygen species that subsequently attack the organic compounds (RH) present in the wastewater by the mechanism shown in Equation (1) [3].



Free radicals (hydroxyl radicals) are molecules that contain an unpaired electron, so they are highly unstable and immediately react with any other existing molecules to acquire the missing electron [4]. Several variables affect the behavior of the process such as H_2O_2 concentration, solution pH, concentration, photocatalyst, operation time, type of ultraviolet light, and the initial concentration of the contaminant [5].

It has been determined that C-type UV light, which has wavelengths between 200 and 300 nm and energies between 4 and 5 eV, is highly efficient in the generation of hydroxyl radicals when emitted over semiconducting metal-containing catalysts such as titanium dioxide or iron oxide and in the presence of an electron acceptor [3]. Furthermore, combination of those semiconductors has shown improved photocatalytic activity particularly for dye discoloration and mineralization. Mancuso et al. [6] determined that TiO_2 , although efficient towards crystal violet dye discoloration, was inefficient in the mineralization of the crystal violet. However, doping with Fe leads, instead, to relevant total organic carbon (TOC) removal of crystal violet from aqueous solutions within 180 min under visible irradiation.

Recently, many performances improving photocatalyst synthesis techniques have been reported, including doping schemes, hydrothermal heterostructuring, electrochemical preparation, sol-gel, and micro emulsion, among others [7]; developing materials with enhanced surface area, controlled morphology and tune controlled band-gap. However, many of these techniques are costly, generate a small amount of material, could produce hazardous byproducts and require high-energy and economic expenditure to achieve the desired properties such as ferrous ion or titanium dioxide doping on specific structures [8].

Natural mineral composites are known to present photoreactive and reactive compounds such as titanium dioxide and ferrous oxide in their structure; among those minerals, magnetite, limonite, ilmenite, and hematite, could be found, among others [9], which in some cases are raw materials to obtain products of higher purity. According to Tang et al. [10], among those mineral composites, ilmenite has a potential worth studying since it can be used in composite materials for the photocatalytic destruction of organic contaminants.

Several researchers have assessed ilmenite as photocatalyst for organic pollutant degradation; Pataquiva-Mateus et al. [11] determined that degradation of Orange II was obtained by dark Fenton during the first 7 h of reaction reaching 90% of COD removal. Similarly, Garcia-Munoz et al. [12] discovered that a catalytic wet peroxide oxidation—photo as-

sisted process using ilmenite as low-cost catalyst—successfully accomplished sulfonamides degradation and mineralization between 35% and 85%.

Most studies focus on model wastewater degradation with controlled concentration of organic pollutants, mainly to obtain degradation pathways and kinetics; however, real wastewater has not been addressed deeply, leaving uncertainty of ilmenite potential applicability on actual processes.

The present work evaluated the use of ilmenite in its natural state as a photocatalyst for the photocatalytic degradation of dyes present in real clinical laboratory wastewater produced during Gram staining, Ziehl-Neelsen staining, and Wright staining procedures. Ilmenite was characterized using X-ray diffraction analysis, N₂ adsorption, X-ray fluorescence, scanning electron microscopy (SEM) and energy dispersive spectroscopy Elemental. Clinical laboratory wastewater was characterized following the environmental parameters established by local regulations. Photocatalytic tests were carried out by adding ilmenite and hydrogen peroxide to the wastewater solution in a 200 mL quartz reactor located inside a dark chamber, composed of 10 UV light-emitting lamps. The effect of ilmenite loading, light wavelength, ilmenite particle size, and its reliability upon reuse were evaluated.

2. Materials and Methods

2.1. Clinical Laboratory Wastewater Characterization

The clinical laboratory wastewater was obtained from the *central de procesamiento de laboratorio clínico—compensar E.P.S.*, a local health service provider from Bogotá, Colombia. Wastewater was characterized by an accredited laboratory in ISO 17025:2017 according to local regulations [13] measuring chemical oxygen demand, biochemical oxygen demand, pH, phenol content, total suspended solids, methylene blue active substances and settleable solids. Table 1 summarizes results of wastewater characterization.

Table 1. Clinical laboratory wastewater characterization.

Parameter	Undiluted	Diluted 5% (v/v)
COD (mg/L)	27,400	5240
BOD ₅ (mg/L)	5200	N/A
pH (units)	6.75	3.84
Phenols (mg/L)	5.4	N/A
TSS (mg/L)	242	N/A
MBAS (mg/L)	<0.4	N/A
SS (mg/L)	<0.5	N/A

Likewise, local wastewater regulations [13] sets the wavelengths of 436, 525 and 620 nm as absorbance references for color measurement of wastewater discharge. UV–Vis spectrum of clinical laboratory wastewater is shown in Figure 1; peaks at 540 nm and 660 nm are identified, corresponding to crystal violet and methylene blue, respectively. The highest absorbance peak obtained was at 0.8 in the 500 and 550 nm wavelength range; therefore, 525 nm wavelength was selected as a reference value to track the degradation process in order to follow local regulation guidelines for color parameter in wastewater.

Undiluted sample transmittance is in the order of 0.025%, meaning only a small fraction of incident radiation penetrates the 10 mm pathlength of the rectangular UV–Vis cell used for the analysis. A reference peak of 525 nm wavelength is well developed, and sample transmittance sample increased up to 18%.

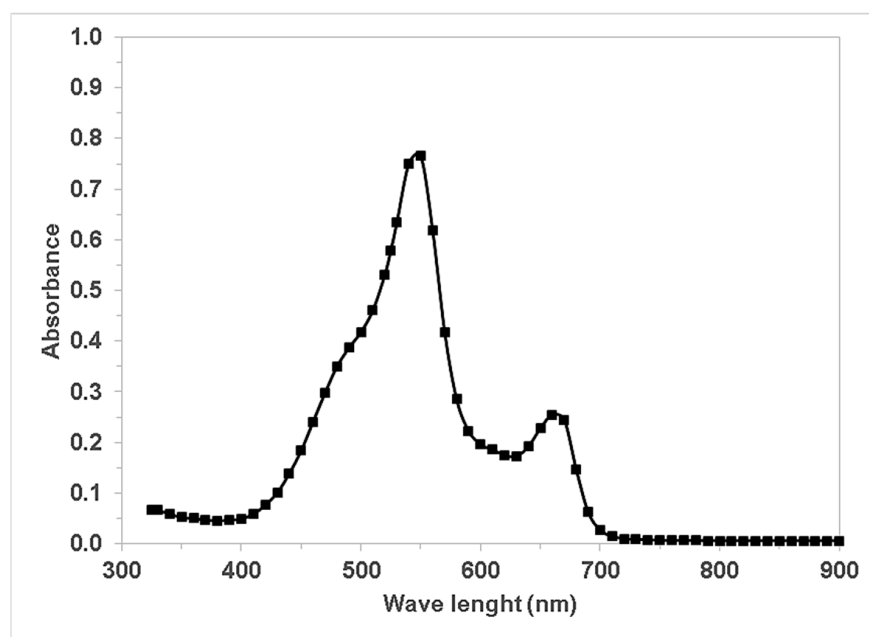


Figure 1. UV-Vis spectrum of the clinical laboratory wastewater diluted sample.

An increase in irradiation energy emitted to the solution allowed UV light type C (254 nm) to be an adequate source to generate the “hollow-electron” pair on catalyst surface. Based on the above, wastewater was diluted to 5% (*v/v*) in distilled water as reference for ilmenite performance evaluation as a photocatalyst.

2.2. Ilmenite Characterization

Ilmenite powdered samples were analyzed with X-ray diffraction (XRD) using a Panalytical X'pert Pro MPD diffractometer under $\text{CuK}\alpha$ radiation working at 30 kV and 50 mA. The obtained XRD data were analyzed using Jade 5 Software (from 5 Sir Gil Simpson Dr, Christchurch, New Zealand) based on the ICDD (International Center for Diffraction Data) database. XRF analysis was performed on a Philips MagixPro PW-2440 X-ray fluorescence spectrophotometer, equipped with a rhodium tube with a maximum power of 4 kW, whose sensitivity of heavy metal elements is 200 ppm. The total surface area was measured by the adsorption of N_2 at 77 K, using a NOVA e-Series surface area analyzer (Quantachrome Absorb-1, Boynton Beach, FL, USA). A Tescan Model Vega 3 scanning electron microscope operating at 20 kV equipped with energy-dispersive spectroscopy (EDS) detection probe was used to evaluate particle surface morphology and composition.

2.3. Experimental Reaction Process

Discoloration process measurement (A/A_0) was determined using the spectrophotometric technique, measuring wastewater absorbance during reaction (A) and comparing it with initial wastewater absorbance (A_0). Wastewater discoloration reaction was carried out in a 200 mL quartz glass located inside an aluminum box with internal illumination. Initial wastewater volume was maintained at 100 mL. A 30% hydrogen peroxide solution was used as electron acceptor, concentration was maintained constant at 10 mM in all experiments using this reactive. Sunlight and visible white light (400 to 700 nm range) effect was executed with the same quartz glass located outside the aluminum box. Agitation was carried out using a Heidolph model MR 3001 magnetic stirring plate (Figure 2), every half hour a 10 mL aliquot was taken to measure absorbance and pH of wastewater, a 5 min centrifugation process was executed previous to measurement to eliminate suspended solids generated by ilmenite agitation inside the solution, avoiding solid interference with the absorbance reading. Absorbance was measured in a Thermo Fisher Scientific reference Genesis 20 model 4001/4 spectrophotometer at a wavelength of 525 nm. pH was deter-

mined in an Orion model SA520 pH meter. Type C—UV light was (254 nm) generated by 10 Sylvania model 7 W lamps and type A UV light was generated by 10 JeneralTek® model F8T5-BLB 7 W lamps located inside the box.

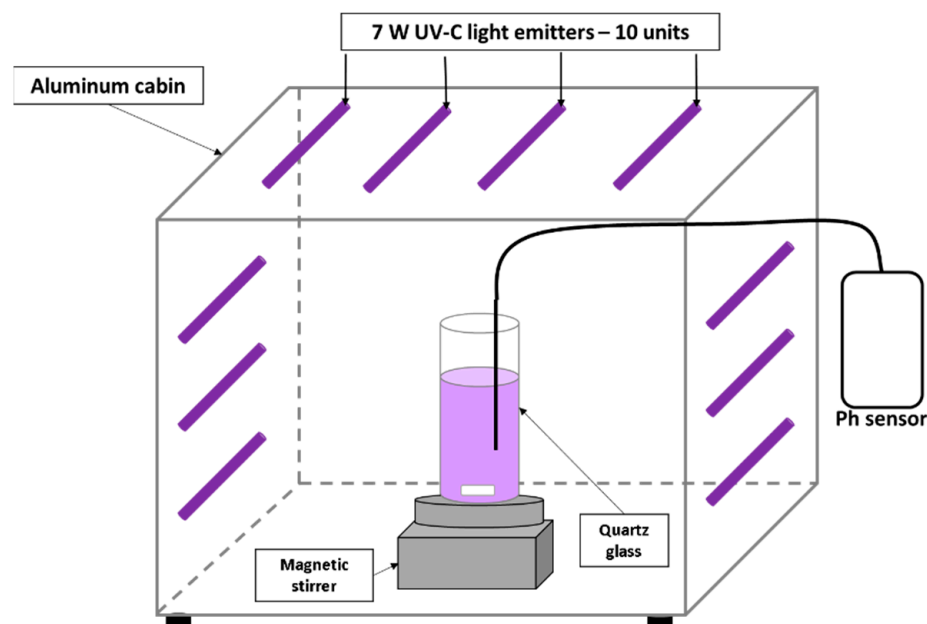


Figure 2. Experimental setup for photocatalytic dye degradation.

Finally, discoloration blanks were performed on the wastewater solution using only hydrogen peroxide at the 10 mM concentration (oxidation), ilmenite at the load with the best color degradation (ilmenite catalysis), UV-C light radiation (photolysis), and ilmenite with ultraviolet light (photocatalysis without hydrogen peroxide) to compare their performance against the photocatalytic discoloration process.

Reaction parameter values were obtained from different literature sources in which it has been determined that similar conditions allows complex organic substances degradation such as nitro aromatics, aromatic carboxylic acids, aromatic carboxylic acids, nitro aromatic acids, aromatic carboxylic acids [14], aromatic carboxylic acids, uracil [15], azo dyes [16], and triphenylmethane-derived dyes [17], thus validating the use of these parameters for the accurate evaluation of the reaction behavior. Ilmenite stability was evaluated by performing degradation cycles.

3. Results

3.1. Ilmenite Characterization

From XRF analysis results (Table 2), it is possible to identify titanium dioxide and iron (III) oxide as the main ilmenite constituents (close to 42% in weight, respectively). Other relevant constituents are silicon dioxide and aluminum oxide (close to 1% and 2% weight, respectively). Some minor constituents are vanadium and manganese oxide, among others. Because ilmenite is usually in sandbanks, it is very common to find impurities such as silicon dioxide because of sediments carried by water currents to the mining sites. The presence of magnesium is also common in ilmenite minerals, and it can vary depending on the mining site. However, the amounts of iron and titanium are representative of ilmenite and allow us to identify that the sample used corresponds to this mineral.

Surface area of the ilmenite was determined using BET equation and data from N_2 isotherms. Figure 3 shows X-ray diffraction patterns for the sample used it can be noticed a complex mixture of mainly ilmenite ($FeTiO_3$, JCPDS No. 29-733), rutile (TiO_2 , JCPDS No. 21-1276), and silicon dioxide (SiO_2 , JCPDS No. 1-88-2487), which is in concordance with the results obtained by XRF. As evidenced by X-ray fluorescence, the sample has impurities mainly represented by silicon dioxide, which has a hexagonal structure and

coincides with the 2θ peaks located at 20.8° , 26.6° , and 50.1° for reference standard 1-88-2487 of Silicon dioxide confirming the presence of this structure within the sample.

Table 2. XRF results for ilmenite.

Element or Compound	(Weight %)
Fe ₂ O ₃	42.645
TiO ₂	41.250
SiO ₂	12.273
Al ₂ O ₃	2.009
MnO	0.914
V	0.198
MgO	0.167
K ₂ O	0.137
Zr	0.105
P ₂ O ₅	0.101
Na ₂ O	0.090
CaO	0.060
Cl	0.020
Nb	0.012
Zn	0.010
S	0.009

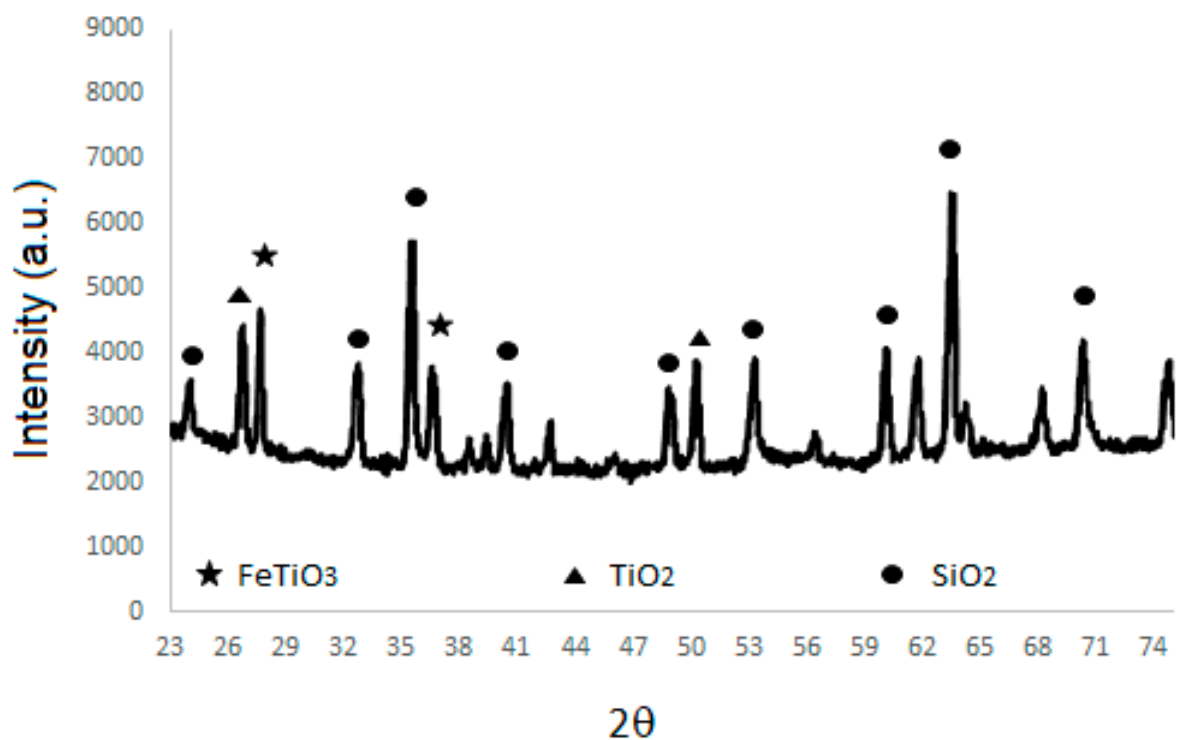


Figure 3. X-ray diffraction pattern of ilmenite.

Figure 4a shows an SEM picture of the ilmenite; the material contains mainly 100-to-400-micron amorphous particles, but some smaller particles can be observed. This type of particle size distribution was observed in several SEM pictures.

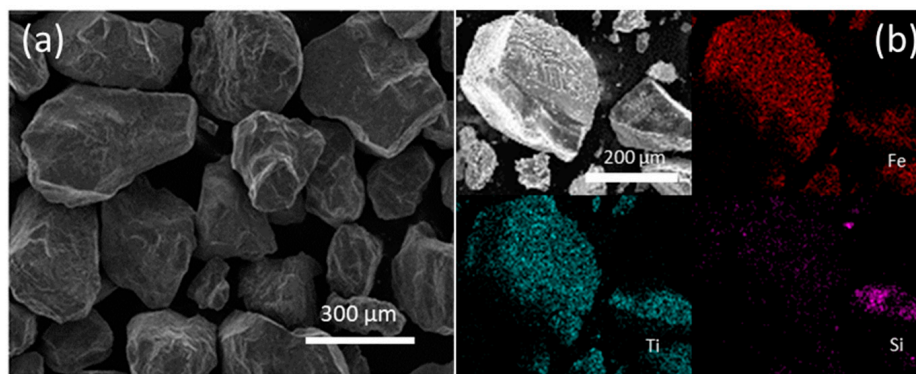


Figure 4. (a) SEM picture of ilmenite sample, (b) EDS mapping analysis of ilmenite sample.

3.2. Experimental Reaction Process

3.2.1. Effect of Ilmenite Concentration

Figure 5 shows the discoloration and pH behavior of the wastewater solution for different loads of ilmenite versus time.

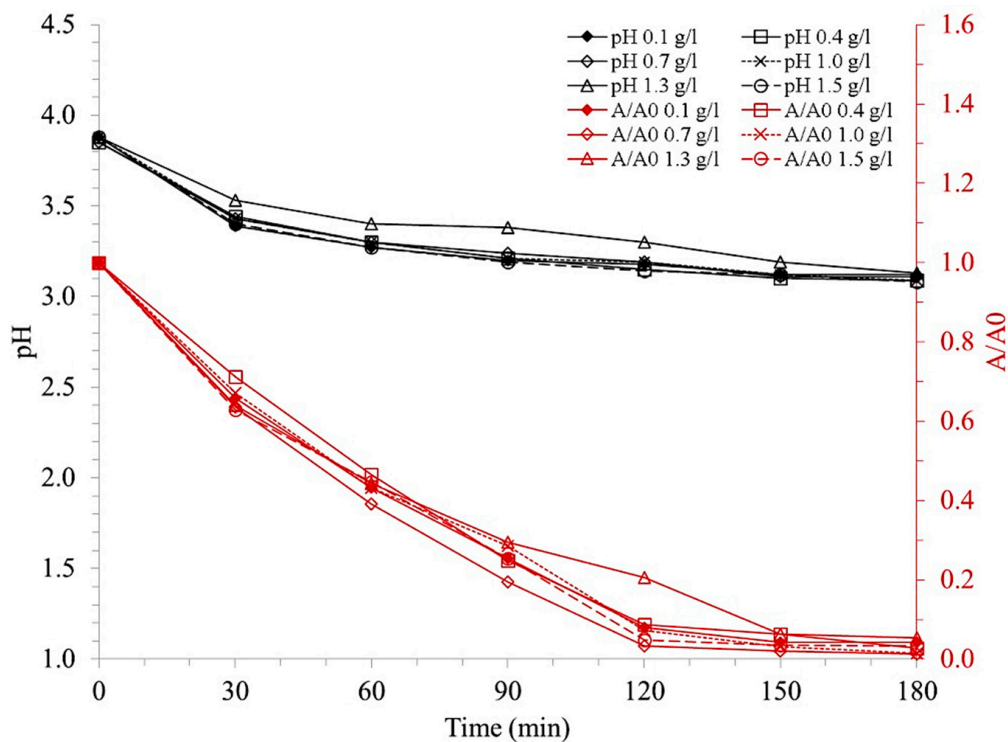


Figure 5. Effect of ilmenite loading on discoloration (A/A_0) and pH. ($[H_2O_2] = 10 \text{ mM}$, $pH_0 = 3.8$, UV-C Light).

On the other hand, Figure 5 shows that a >90% discoloration was obtained after a 3 h reaction process. Likewise, a 50% discoloration was obtained just after a 1 h reaction. A 0.7 g/L ilmenite load showed the best reaction performance by reaching 97% at 2 h reaction time and 98.6% at 3 h reaction time.

3.2.2. Effect of Light Type

Ilmenite behavior for dye degradation under different sources of light irradiation was evaluated, experiments were carried out using commercial visible white light, sunlight, ultraviolet light type A and ultraviolet light type C, using the same conditions of hydrogen peroxide concentration, best performance ilmenite load, reaction time and initial pH. Results are presented in Figure 6.

Figure 6 shows that UV-A light presented better performance than sunlight and visible light photocatalytic process; however, only 20% discoloration was obtained after a 3 h reaction, which significantly differs from the 98% discoloration obtained when UV-C light was used.

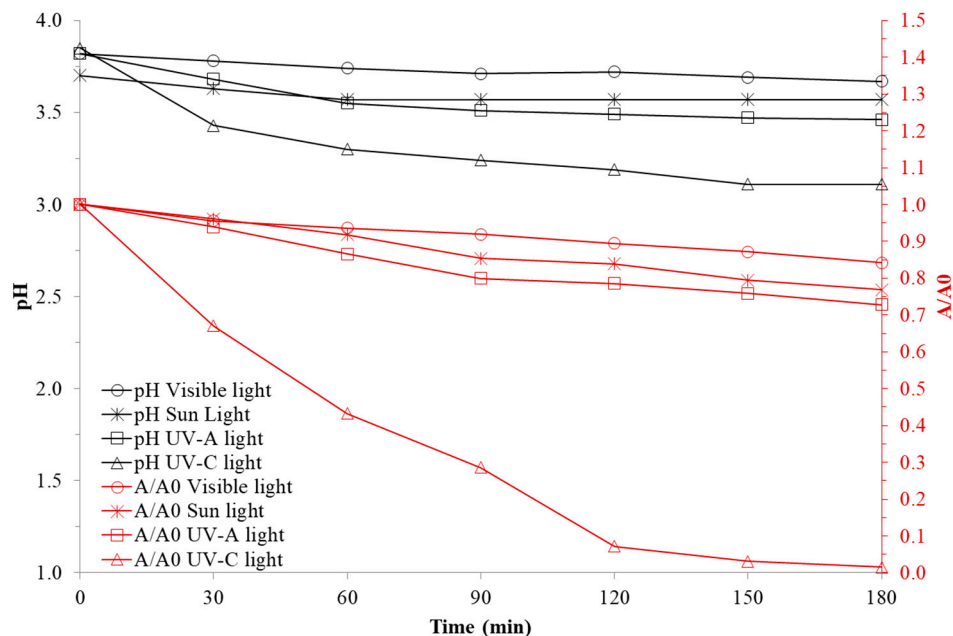


Figure 6. Effect of the type of light source on discoloration and pH ($[H_2O_2] = 10 \text{ mM}$, $pH_0 = 3.8$, Ilmenite loading = 0.7 g/L).

3.2.3. Effect of Ilmenite Particle Size

Ilmenite particle size effect was studied after ilmenite concentration effect analysis on wastewater discoloration. Ilmenite was crushed and sieved in an ASTM E-11 mesh system, retained content in each mesh was weighed and particle size distribution was identified. Results are presented in Figures 7 and 8.

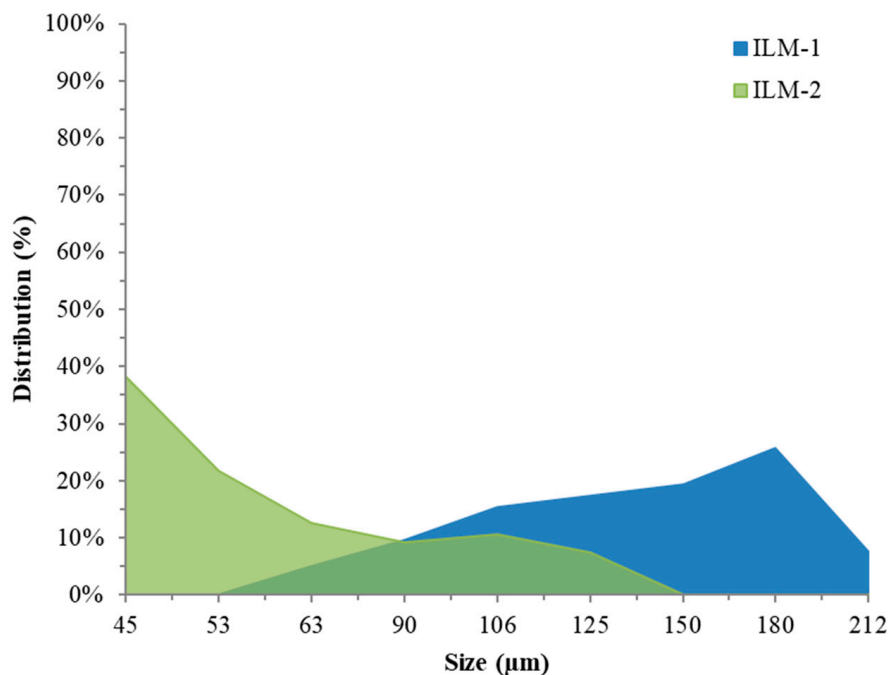


Figure 7. Particle size distribution in ASTM E-11 mesh for ilmenite.

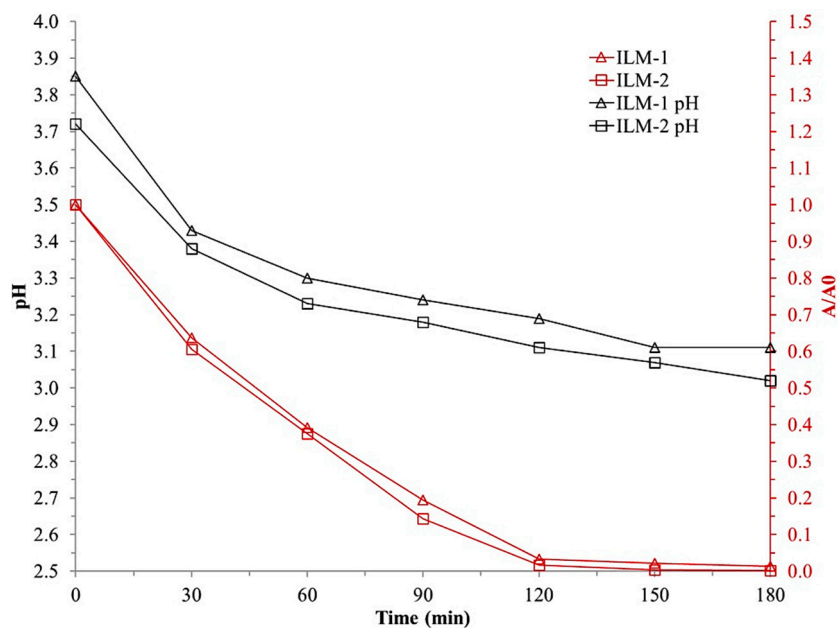


Figure 8. Effect of ilmenite particle size on discoloration ($[H_2O_2] = 10 \text{ mM}$, $pH_0 = 3.8$, UVC, Ilmenite loading = 0.7 g/L).

Figure 7 represents the percentage size distribution found for the crushed sample, as the sample was sieved together with uncrushed material it was determined that size 1 (ILM-1) corresponds to ilmenite in its natural state which has a particle size between around 100 and 400 μm ; subsequently, size 2 (ILM-2) was obtained, which corresponds to the interval between around 40 and 100 μm ; particle size of less than 50 μm accounts for 60% of total particle size distribution after the crushing process.

3.2.4. Ilmenite Stability

To fully evaluate ilmenite performance in wastewater photocatalytic discoloration process, four consecutive tests were carried out reusing ilmenite. Results are shown in Figure 9.

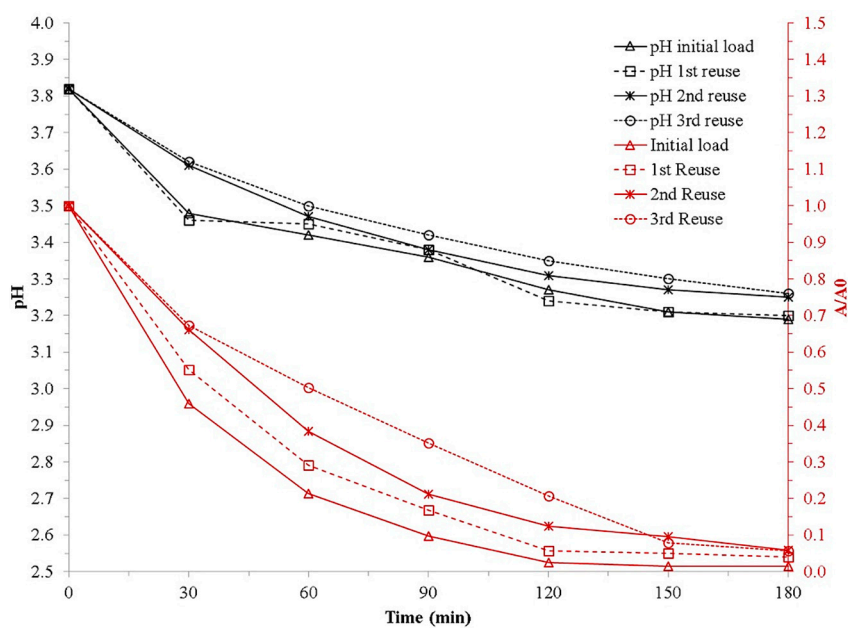


Figure 9. Ilmenite stability after 4 tests (3 reuses) ($[H_2O_2] = 10 \text{ mM}$, $pH_0 = 3.8$, UVC light).

The behavior of each of the ilmenite reused is shown in Figure 9, in which the loss of efficiency of the discoloration process is observed as the mineral is reused. Nevertheless, in all cases, discoloration percentages of more than 90% were obtained after 3 h of reaction, indicating that the ilmenite is relatively reliable. The same discoloration behavior can be seen in the behavior of the pH of the wastewater solution, which showed a progressive decrease in acid formation as the material was reused.

4. Discussion

4.1. Ilmenite Characterization

After surface BET area analysis, ilmenite showed around $4 \text{ m}^2/\text{g}$, as well as low micropore areas and volumes. The ilmenite sample generated adsorption/desorption paths with features corresponding to not well-developed type II isotherms, where the average pore size of the sample is mainly in or above the micropore range. Obtained value is relevant when compared with results obtained in other studies, amounting to approximately $6 \text{ m}^2/\text{g}$ [18] and $5 \text{ m}^2/\text{g}$ [19].

EDS elemental mapping for Fe, Ti, and Si is shown in Figure 4b. It confirms that natural ilmenite samples are mainly constituted of Ti and Fe compounds and that its distribution is homogenous in most of the particles. Results also show that Si is not as well-distributed as Ti and Fe, meaning it could probably be a contamination from the mining site.

4.2. Experimental Reaction Process

4.2.1. Effect of Ilmenite Concentration

In Figure 5, loads lower than 0.7 g/L such as 0.1 and 0.4 g/L decreased reaction performance as shown in Figure 5. This could be associated with lower ilmenite concentrations and thus lower availability of active sites to generate the “hole” electron pair responsible electron generation and subsequent electron acceptor reaction, in this case, of hydrogen peroxide, forming the hydroxyl radical.

Ilmenite load increase does not imply an increase in discoloration performance on weight bases; by increasing the ilmenite loading above 0.7 g/L , at a degradation time of 90 min, the performance slightly decreases. Theoretically, an increase in the active sites available to be activated by ultraviolet irradiation would increase the performance of the reaction. This occurs up to the concentration of 0.7 g/L ; however, as ilmenite load increased, discoloration efficiency decreased, mainly because ilmenite particles excess increases wastewater opacity, decreasing UV light flux reaching catalyst particles, and thus photochemical mechanism activation and hydroxyl radical generation.

A 0.8 pH decrease is evidenced during the reaction (Figure 5), which may imply the formation of organic acids. This trend presents consistency with photo-Fenton and photocatalysis reactions in which the generation of hydronium ions is promoted by ferrous iron regeneration in the former and the reaction between water and the valence band “gap” in the latter. For different ilmenite loadings, similar behavior is evidenced in pH change ending between values of 3.08 and 3.12 units. Finally, pollutant degradation was verified by Chemical Oxygen Demand (COD) measurement after a 3 h treatment with 0.7 g/L of ilmenite; a $1270 \text{ mgO}_2/\text{L}$ was obtained, which represents 76% of degradation compared to an initial COD value of $5240 \text{ mgO}_2/\text{L}$ for diluted wastewater to 5% (v/v).

Result allows inferring that discoloration process occurs due to dye aromatic rings breaking, which cause the characteristic purple color of crystal violet. According to Fan et al., crystal violet and triphenylmethane dyes in general follow several degradation paths. The hydroxyl radical attacks the double bond present between the central carbon of the molecule and the carbon of the aromatic ring attached. Once there, the molecule takes the characteristics of a radical and, in the presence of oxygen, it dissociates forming a molecule of 2-methyl aminophenol leaving an aromatic diamine radical which reacts with water to produce an aromatic ketone; from this moment, the hydroxyl radical continues attacking the molecule on the methyl radicals attached to the amine generating formic acid in the process and eliminating the color of the solution [20].

Finally, diluted wastewater treated with an ilmenite loading of 0.7 g/L was spectrally scanned from 325 to 900 nm to compare it with the initial wastewater solution. Figure 10 represents the spectral sweep of initial wastewater solution compared with the final treated solution, clearly showing a complete elimination of the absorbance of the solution in the entire visible spectrum. However, as it approaches the ultraviolet spectrum, the solution begins to show an increase in its absorbance values, which indicates the presence of species resulting from the degradation of the dyes and agrees with the 50% COD degradation value obtained.

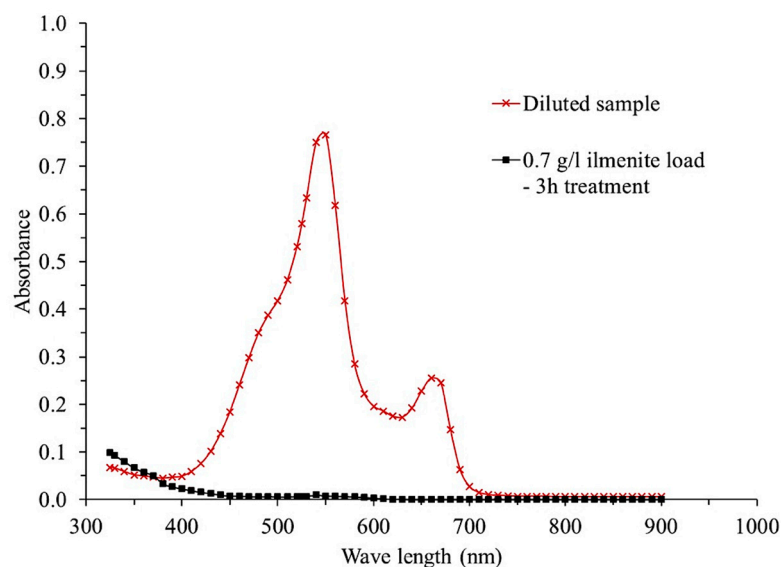


Figure 10. Spectral scan of the diluted wastewater solution before and after the photocatalytic reaction.

4.2.2. Light Type Effect

In Figure 6, differences obtained between UV-A and UV-C light show that the photocatalytic process has the greatest effect on wastewater discoloration, primarily due to the difference in the energies of the photons irradiated at the two wavelengths. UV-A light has a wavelength of approximately 315 to 400 nm, which implies an energy of 3.1 to 3.9 eV, although this energy is close to and can reach the energy of the titanium dioxide band gap (3.2 eV) necessary to generate the hole–electron pair between its valence band and conduction band. However, since ilmenite is natural mineral without further treatment, impurities can prevent all the energy from directly reaching the titanium dioxide particles. Second solution color and high absorbance can prevent the totality of the irradiated light from reaching the titanium dioxide, minimizing the energy with which it reaches the surface of the catalyst and therefore altering the efficiency of the photocatalytic process.

The discoloration of 20% obtained with UV-A light may be because of the photo-Fenton process, which does not require the energy of 3.2 eV necessary to generate the hole–electron pair, since in this case the mechanism works through the regeneration of the ferrous ion by the action of the near-ultraviolet light. During irradiation with UV-C light, a much greater discoloration was obtained, which could be favored by the higher energy intensity of this type of irradiation, which is in the order of 4.14 to 12.0 eV, sufficient energy capable of activating the titanium dioxide and promoting the generation of hydroxyl radicals.

When comparing the results obtained with UV-A light and UV-C light against those obtained by direct photolysis with UV-C light without the use of hydrogen peroxide and photooxidation with UV-C light and with the use of hydrogen peroxide (Figure 11), it can be evidenced that the dye is susceptible to discoloration by direct absorption of UV-C light, however, the effect of the photo-Fenton process with the use of UV-A light can be noted, since a higher percentage of discoloration is obtained than that obtained through direct photolysis. This result may imply that the process that governs the discoloration of the dye when using UV-C light is that of photocatalysis by the action of titanium

dioxide, considering that this type of light has a little incidence on the discoloration of the wastewater solution in a direct way. However, when using hydrogen peroxide for the same ilmenite loading used for the photocatalysis tests together with ultraviolet irradiation Type C, an increase in the percentage of discoloration of the wastewater solution is evidenced, reaching almost 90% at the end of the process. This is mainly because of the production of hydroxyl radicals from the dissociation of hydrogen peroxide by irradiation with high-energy ultraviolet light (Type C); during the process, there is an increase in the discoloration compared to the processes with UV-A light and direct photolysis. This shows that the action of type C ultraviolet light is indispensable for the process. However, the use of ilmenite increases the efficiency of the process by allowing a percentage of discoloration greater than 90% in the three hours of process compared to the 70% discoloration obtained by photo-oxidation. Finally, by performing the direct oxidation processes with hydrogen peroxide and catalysis with ilmenite without the incidence of any type of light (blank tests), it can be corroborated that the discoloration process is highly influenced by type of irradiation source, as shown in Figure 11, in which the oxidation and catalysis curves without irradiation of any type of light do not generate a discoloration of the wastewater solution greater than 10%. These tests show that a photocatalytic process is being carried out, in which the synergy achieved between ilmenite, hydrogen peroxide and C-type ultraviolet light irradiation is evident.

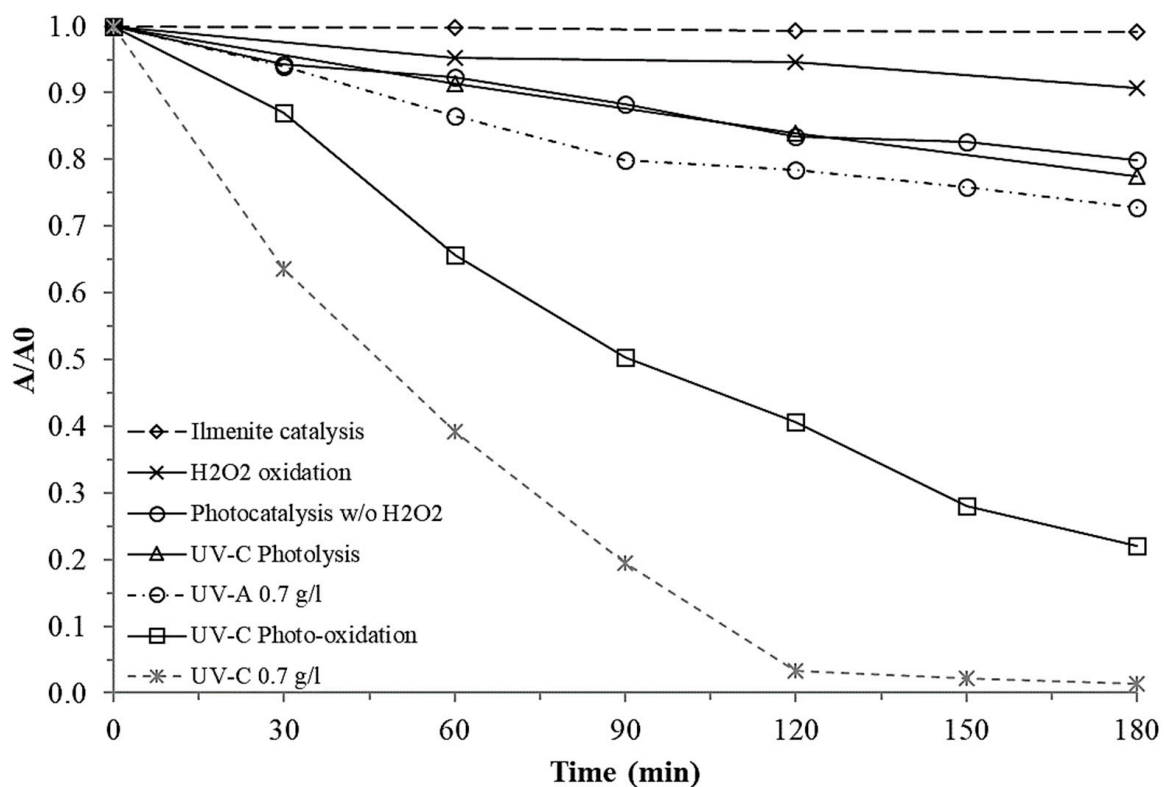


Figure 11. Comparison between ilmenite catalysis without H_2O_2 and light source, H_2O_2 oxidation, UV-C direct photolysis, UV-C- H_2O_2 photo-oxidation, UV-A photocatalysis, UV-C photocatalysis. ($[H_2O_2] = 10$ mM, $pH_0 = 3.8$, Ilmenite loading = 0.7 g/L).

4.2.3. Ilmenite Particle Size Effect

Photocatalytic test was performed for the ILM-2 ilmenite. The conditions of this test were: ilmenite loading of 0.7 g/L, ultraviolet light type C, 10 mM concentration of hydrogen peroxide, 5% dilution (v/v) of the wastewater solution in distilled water, and initial pH of 3.8 units. Figure 8 illustrates wastewater discoloration behavior by absorbance measuring

at 525 nm. It can be noticed that particle size reduction obtained with ILM-2 sample up to the interval of 45 to 125 μm allows obtaining 100% discoloration in the 3 h reaction time.

When reviewing the pH behavior during the reaction, it is evident that the solution treated with ILM-1 presented a pH one unit higher than the solution treated with ILM-2, which allows inferring that the acidification of the solution is promoted during the discoloration when the particle size of the ilmenite is reduced. The ILM-2 degradation shows an interesting behavior; it reaches comparable or higher discoloration than the ILM-1 sample at shorter times (see Figure 8).

To verify the percentage of degradation obtained with the particle size reduction, COD analysis was performed on the wastewater solution obtained from the treatment with ilmenite crushed to ILM-2 size. A 1120 mgO_2/L COD value was obtained, corresponding to a 78.6% of degradation, from the initial value of the wastewater solution (5240 mgO_2/L), indicating that the reduction in particle size, in addition to improving the discoloration performance, also presents an increase in the percentage of degradation of the wastewater solution.

The improved performance on the size-reduced ilmenite can be explained by the BET surface area analysis. The uncrushed ilmenite presents a surface area of 4 m^2/g indicating a low surface area and low porosity; when the analysis was performed on the crushed ilmenite, a value of 9 m^2/g was obtained. The increase on the surface area in the ilmenite also increases the number of available active sites where the photocatalytic reactions occur.

4.2.4. Ilmenite Reuse Test

The analysis of the degradation of the dyes showed the same behavior of reduction in the efficiency of the process. The final COD of the wastewater solution treated with the third reuse of the catalyst presented a value of 1520 mgO_2/L , a value higher than the 942 mgO_2/L obtained for the wastewater solution treated with ilmenite used only once.

The loss of efficiency may be due to a progressive inactivation of the ilmenite material with intermediate species formed during discoloration such as carbonates, malic acid, and hydroquinone, among others, originating from the degradation of phenols, which act as traps for the photo catalytically generated "holes" [21]. Additionally, because the waste solution is real wastewater, the presence of solvents and acids used in the staining process can slow down the discoloration process as they adsorb on the surface of the catalyst, species such as acetonitrile and various alcohols have a significant inhibitory effect on the decolorizing capacity of titanium dioxide [22].

5. Conclusions

A high concentration of oxidizable organic matter was identified in the clinical laboratory wastewater. The discoloration process of the wastewater solution containing dyes was carried out using Ilmenite as a catalyst, which presented the best discoloration performance when irradiated with ultraviolet light type C (254 nm). Type C ultraviolet light was identified as the light source with the best performance on the discoloration due to the activation of the "hole"–electron pair on the surface of the titanium dioxide. This could be established because the irradiation with type A ultraviolet light did not show a discoloration higher than 30%, which allowed establishing that the semiconductor activation was not achieved; in this case, the discoloration was carried out by the action of the photo-Fenton process, which does not require such high energies for its execution. The characterization of the mineral allowed us to identify the presence of titanium dioxide and ferrous oxide in a wide proportion, as well as the presence of silicon dioxide impurities which were found as complete grains and as an impurity within the FeTiO_3 hexagonal system of the ilmenite. The X-ray diffraction characterization allowed us to identify the presence of a small proportion of the rutile phase in the ilmenite structure—the FeTiO_3 phase, the one with the highest presence in the structure of the mineral. An optimum in the ilmenite load was evidenced when analyzing its effect on the process. An increase above 0.7 g/L load generates an inhibition process, mainly due to the increase in the concentration of catalyst particles and

impurities that dull the solution and decrease the intensity with which the irradiated light acts on other catalyst particles. Similarly, a decrease in particle size promoted an increase in the specific area of the ilmenite and consequently a higher percentage of discoloration of the wastewater solution.

It was possible to establish that ilmenite is stable after four uses in the discoloration process of the wastewater solution, obtaining, in all cases, discoloration percentages higher than 90% after 3 h of irradiation. The loss of efficiency occurs mainly due to the contamination of the catalyst surface with intermediate organic substances generated by the discoloration.

Author Contributions: Conceptualization, H.R.Z.R. and J.H.R.F.; methodology, S.D.C.C.; formal analysis, H.R.Z.R., J.H.R.F. and S.D.C.C.; investigation, S.D.C.C.; resources, J.H.R.F.; writing—original draft preparation, H.R.Z.R.; writing—review and editing, H.R.Z.R. and J.H.R.F.; supervision, J.H.R.F.; project administration, J.H.R.F. All authors have read and agreed to the published version of the manuscript.

Funding: This research received no external funding.

Informed Consent Statement: Not applicable.

Data Availability Statement: Data supporting reported can be requested through email jhramirezfra@unal.edu.co.

Conflicts of Interest: The authors declare no conflict of interest.

References

1. IDEAM. *Informe Nacional de Residuos o Desechos Peligrosos en Colombia*; Ministerio de Ambiente y Desarrollo Sostenible: Bogotá, Colombia, 2017.
2. Herney-Ramirez, J.; Lampinen, M.; Vicente, M.A.; Costa, C.A.; Madeira, L.M. Experimental Design to Optimize the Oxidation of Orange II Dye Solution Using a Clay-Based Fenton-like Catalyst. *Ind. Eng. Chem. Res.* **2008**, *47*, 284–294. [[CrossRef](#)]
3. Herney-Ramirez, J.; Vicente, M.A.; Madeira, L.M. Heterogeneous Photo-Fenton Oxidation with Pillared Clay-Based Catalysts for Wastewater Treatment: A Review. *Appl. Catal. B Environ.* **2010**, *1–2*, 10–26. [[CrossRef](#)]
4. Gottschalk, C.; Libra, J.A.; Sau, A. *Ozonization of Water and Wastewater: A Practical Guide to Understanding Ozone and Its*, 2nd ed.; Wiley-Vch Verlag GmbH & Co.: Weinheim, Germany, 2010.
5. Faisal, M.; Malick, T.; Muneer, M. Photocatalysed Degradation of Two Selected Dyes in UV-Irradiated Aqueous Suspensions of Titania. *Dye. Pigment.* **2007**, *72*, 233–239. [[CrossRef](#)]
6. Mancuso, A.; Blangetti, N.; Sacco, O.; Freyria, F.S.; Bonelli, B.; Esposito, S.; Sannino, D.; Vaiano, V. Photocatalytic Degradation of Crystal Violet Dye under Visible Light by Fe-Doped TiO₂ Prepared by Reverse-Micelle Sol–Gel Method. *Nanomaterials* **2023**, *13*, 270. [[CrossRef](#)] [[PubMed](#)]
7. Mudhoo, A.; Paliya, S.; Goswami, P.; Singh, M.; Lofrano, G.; Carotenuto, M.; Carraturo, F.; Libralato, G.; Guida, M.; Usman, M.; et al. Fabrication, Functionalization and Performance of Doped Photocatalysts for Dye Degradation and Mineralization: A Review. *Environ. Chem. Lett.* **2020**, *18*, 1825–1903. [[CrossRef](#)]
8. Ozkan, U. *Design of Heterogeneous Catalysts New Approaches Based on Synthesis, Characterization and Modeling*; Wiley: Hoboken, NJ, USA, 2009.
9. U.S. Environmental Protection Agency. *Extraction and Beneficiation of Ores and Minerals*; EPA: Washington, DC, USA, 1994; NTIS PB94-195203.
10. Tang, X.; Tang, R.; Xiong, S.; Zheng, J.; Li, L.; Zhou, Z.; Gong, D.; Deng, Y.; Su, L.; Liao, C. Application of Natural Minerals in Photocatalytic Degradation of Organic Pollutants: A Review. *Sci. Total Environ.* **2022**, *812*, 152434. [[CrossRef](#)] [[PubMed](#)]
11. Pataquiva-Mateus, A.Y.; Zea, H.R.; Ramirez, J.H. Degradation of Orange II by Fenton Reaction Using Ilmenite as Catalyst. *Environ. Sci. Pollut. Res.* **2017**, *24*, 6187–6194. [[CrossRef](#)] [[PubMed](#)]
12. Garcia-Muñoz, P.; Pliego, G.; Zazo, J.A.; Bahamonde, A.; Casas, J.A. Sulfonamides Photoassisted Oxidation Treatments Catalyzed by Ilmenite. *Chemosphere* **2017**, *180*, 523–530. [[CrossRef](#)] [[PubMed](#)]
13. Ministerio de Ambiente y Desarrollo Sostenible. *Resolución 631 de 2015 “Por la Cual se Establecen los Parámetros y los Valores Límites Máximos Permisibles en los Vertimientos Puntuales a Cuerpos de Aguas Superficiales y a los Sistemas de Alcantarillado Público y se Dictan otras Disposiciones*; Ministerio de Ambiente y Desarrollo Sostenible: Bogotá, Colombia, 2015.
14. Hakki, A.; Dillert, R.; Bahnemann, D. Photocatalytic Conversion of Nitroaromatic Compounds in the Presence of TiO₂. *Catal. Today* **2009**, *144*, 154–159. [[CrossRef](#)]
15. Bahnemann, W.; Muneer, M.; Haque, M.M. Titanium Dioxide-Mediated Photocatalysed Degradation of Few Selected Organic Pollutants in Aqueous Suspensions. *Catal. Today* **2007**, *124*, 133–148. [[CrossRef](#)]

16. Wang, J.; Zhao, G.; Zhang, Z.; Zhang, X.; Zhang, G.; Ma, T.; Jiang, Y.; Zhang, P.; Li, Y. Investigation on Degradation of Azo Fuchsine Using Visible Light in the Presence of Heat-Treated Anatase TiO₂ Powder. *Dye. Pigment.* **2007**, *75*, 335–343. [[CrossRef](#)]
17. Xu, H.-Y.; Zheng, Z.; Mao, G.-J. Enhanced Photocatalytic Discoloration of Acid Fuchsine Wastewater by TiO₂/Schorl Composite Catalyst. *J. Hazard. Mater.* **2010**, *175*, 658–665. [[CrossRef](#)] [[PubMed](#)]
18. García-Muñoz, P.; Pliego, G.; Zazo, J.A.; Bahamonde, A.; Casas, J.A. Ilmenite (FeTiO₃) as Low Cost Catalyst for Advanced Oxidation Processes. *J. Environ. Chem. Eng.* **2016**, *4*, 542–548. [[CrossRef](#)]
19. Mehdilo, A.; Irannajad, M. Comparison of Microwave Irradiation and Oxidation Roasting as Pretreatment Methods for Modification of Ilmenite Physicochemical Properties. *J. Ind. Eng. Chem.* **2016**, *33*, 59–72. [[CrossRef](#)]
20. Fan, H.-J.; Huang, S.-T.; Chung, W.-H.; Jan, J.-L.; Lin, W.-Y.; Chen, C.-C. Degradation Pathways of Crystal Violet by Fenton and Fenton-like Systems: Condition Optimization and Intermediate Separation and Identification. *J. Hazard. Mater.* **2009**, *171*, 1032–1044. [[CrossRef](#)] [[PubMed](#)]
21. Carp, O.; Huisman, C.L.; Reller, A. Photoinduced Reactivity of Titanium Dioxide. *Prog. Solid State Chem.* **2004**, *32*, 33–177. [[CrossRef](#)]
22. Epling, G.A.; Lin, C. Investigation of Retardation Effects on the Titanium Dioxide Photodegradation System. *Chemosphere* **2002**, *46*, 937–944. [[CrossRef](#)] [[PubMed](#)]

Disclaimer/Publisher’s Note: The statements, opinions and data contained in all publications are solely those of the individual author(s) and contributor(s) and not of MDPI and/or the editor(s). MDPI and/or the editor(s) disclaim responsibility for any injury to people or property resulting from any ideas, methods, instructions or products referred to in the content.